AUGUST 01 2008

Noise reduction in tunnels by hard rough surfaces

Ming Kan Law; Kai Ming Li; Chun Wah Leung

J. Acoust. Soc. Am. 124, 961–972 (2008)
https://doi.org/10.1121/1.2932255

Noise reduction in tunnels by hard rough surfaces

Ming Kan Law
Department of Mechanical Engineering, The Hong Kong Polytechnic University, Hung Hom, Hong Kong

Kai Ming Li[a)]
Ray W. Herrick Laboratories, School of Mechanical Engineering, Purdue University, 140 Martin Jischke Drive, West Lafayette, Indiana 47907-2031

Chun Wah Leung
Department of Mechanical Engineering, The Hong Kong Polytechnic University, Hung Hom, Hong Kong

(Received 2 January 2008; revised 21 April 2008; accepted 30 April 2008)

This paper examines the feasibility of using two-dimensional hard rough surfaces to reduce noise levels in traffic tunnels with perfectly reflecting boundaries. First, the Twersky boss model is used to estimate the acoustic impedance of a hard rough surface. Second, an image source model is then used to compute the propagation of sound in a long rectangular enclosure with finite impedance. The total sound fields are calculated by summing the contributions from all image sources coherently. Two model tunnels are built to validate the proposed model experimentally. Finally, a case study for a realistic geometrical configuration is presented to explore the use of hard rough surfaces for reducing traffic noise in a tunnel which is constructed with hard boundaries.
 [DOI: 10.1121/1.2932255]

PACS number(s): 43.50.Gf, 43.28.Js, 43.20.Mv, 43.20.El [KA] Pages: 961–972

I. INTRODUCTION

Traffic tunnels are widely constructed to convey road and rail traffic worldwide. Reduction in noise in tunnels is a challenging task. The geometrical designs of road traffic or railway tunnels are essentially unfavorable for implementing noise control measures. Large aspect ratios and hard boundary surfaces have led to unevenly distributions of sound fields and tremendous buildup of noise levels due to the effect of multiple reflections from the tunnel walls. The improvement of the acoustic environments in traffic tunnels is an important issue not only for the benefit of the overall noise reductions but also for improving the acoustic performance of public address systems.

There has been considerable research into the physical phenomena of sound propagation in long enclosures.[1] Numerical models, indoor scale-model experiments and full-scale outdoor field measurements were developed for predicting sound pressure levels, reverberation times and other noise metrics in underground stations,[2,3] corridors,[4] road, and railway traffic tunnels.[5–8] Different geometrical acoustic models, the incoherent and coherent approaches, are frequently used in previous studies because of their solutions are usually cast in a relatively simple form for easy numerical implementation. The incoherent model is also known as the energy approach, which has been extensively used in room acoustics and early studies of sound propagation in urban environments.[2–12] In a recent study for predicting sound fields in a street canyon,[13] the incoherent model was found to be accurate if the width of a street is greater than 10 m. Picat *et al.*[14] also showed experimentally that the incoherent model was adequate if the boundary surfaces of a street canyon reflected sound diffusely. On the other hand, the coherent approach is based on a complex image model. Recent studies[15,16] have shown that the coherent model can lead to more accurate predictions of the sound pressure levels and reverberation times in long enclosures because the model takes into account of the interference effect due to different image sources.

In principle, it is possible to apply conventional sound absorption materials on the tunnel walls for noise reduction.[17] However, their use for noise reduction in tunnels poses a health safety problem because of the known aging effects of fiber glass. In addition, tunnel surfaces are usually designed to reduce potential risks of fire hazards and to minimize the costs associated with cleaning and maintenance for the sound absorption materials.

It has been known that a hard rough surface offers incoherent scattering of incoming sound waves. This phenomenon results in the creation of apparent impedances on the hard rough reflecting surfaces.[18–21] Theoretical predictions according to the boundary element formulation, indoor and outdoor measured data have all confirmed the effect on the propagation of sound above a hard rough surface.[22–24] With this information, we wish to examine the effect of deliberate roughening of an otherwise acoustically hard surface on the propagation of sound in tunnels and to explore their potential use for noise reduction.

In Sec. II, we describe the Twersky's boss model and the complex image source model. They are used to describe the effect of hard rough surface on sound reflections and the propagation of sound in long enclosure, respectively. The classical Weyl-van der Pol formula[25] will be used to compute the propagation of sound at near grazing incidence from an image source over a hard rough surface in the tunnels. Section III presents two sets of experimental results carried out;

[a)]Electronic mail: mmkmli@purdue.edu

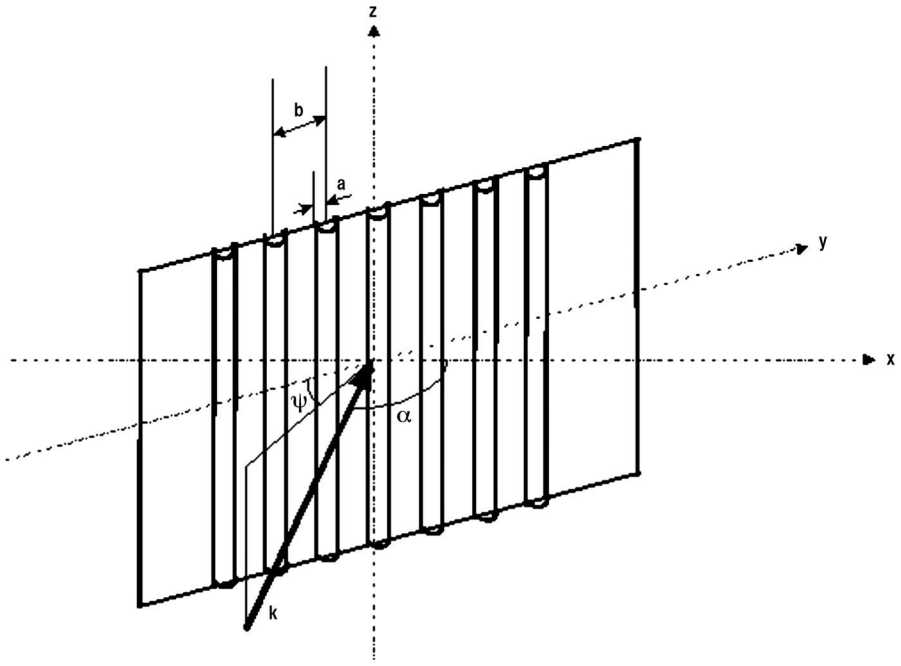

FIG. 1. A schematic diagram to show an incident wave on a rough surface which is made of semicylindrical bosses.

first, in a smaller scale model long enclosure built in an anechoic chamber and, second, a larger one-tenth scale model tunnel mounted outdoors for validating the theoretical formulations. Numerical simulations of the sound fields in a road traffic tunnel and the use of hard rough surfaces for noise reduction are presented in Sec. IV. Concluding remarks and discussions are offered in the last section.

II. THEORY

A. Twersky's boss theory for hard rough planes

Twersky's model describes the coherent reflection and incoherent scattering of sound from a rigid surface embedding with semicylindrical bosses. His mathematical formulation takes into account the interaction of scattering sounds between the neighboring bosses, which enables the use of an effective impedance to predict the coherent reflection from a rough surface. Twersky's model can be applied to calculate the plane wave reflection coefficient of a hard rough surface. Using the notations consistent with the previous publications,[23] the main results for a hard rough surface are stated in the following paragraphs although the details of Twersky's theory can be found elsewhere.[18]

Consider a rough surface that is made by spacing arrays of semicylindrical bosses either periodically or nonperiodically over a rigid plane. A plane wave is incident on this hard rough surface locating at the plane $x=0$ (see Fig. 1 for the schematic diagram of the problem). According to the two-dimensional Twersky boss model, the effective admittance β_e (normalized with air) of the hard rough surface can be evaluated by

$$\beta_e = \eta_{2D} - i\xi_{2D}, \tag{1}$$

where

$$\eta_{2D}(\alpha,\varphi) = \frac{mk^3\pi^2a^4}{8}(1-W^2)\left\{(1-\sin^2\alpha\sin^2\varphi)\left[1 + \left(\frac{\delta^2}{2}\cos^2\varphi - \sin^2\varphi\right)\sin^2\alpha\right]\right\}, \tag{2}$$

$$\xi_{2D}(\alpha,\varphi) = kV[-1 + (\delta\cos^2\varphi + \sin^2\varphi)\sin^2\alpha], \tag{3}$$

where $k(\equiv\omega/c)$ is the wave number, with ω and c as the angular frequency and speed of sound in air, respectively. The parameters η_{2D} and ξ_{2D} are the incoherent scattering loss and multipole coupling terms, respectively, α is the angle of incidence measured from the normal of the rigid plane, and φ is the azimuthal angle between the wave vector and the axes of semicylinders. $V=m\pi a^2/2$ represents the total raised volume per unit area of the bosses, where m is the number of semicylinders per unit length $(m=1/b)$ and $\delta=2/(1+I)$ is a measure of the coupling effects between the semicylinders. The parameters a and b are the radius and mean center-to-center spacing of the semi-cylinders, respectively. If the semicylindrical bosses are periodically arranged, then I can be approximated by $(\pi a)^2/3b^2$. Otherwise, it is given by

$$I \cong \begin{cases} 2W(1+0.307W+0.137W^2)(a^2/b^2) & \text{for } W<0.8 \\ \dfrac{\pi^2}{3}\left[1-\dfrac{2(1-W)}{W}\right]+6\dfrac{(1-W)^2}{W^2}\left[\dfrac{\pi^2}{6}+1.202\right](a^2/b^2) & \text{for } W\geqslant 0.8, \end{cases} \tag{4}$$

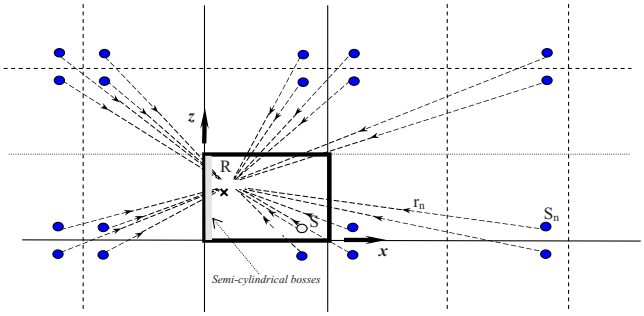

FIG. 2. (Color online) Typical image sources formed in a rectangular enclosure by multiple reflections on the boundary surfaces.

where $W=mb^*=b^*/b$, b^* is the minimum center-to-center separation between two adjacent semicylinders. The term $(1-W)^2$, which is also known as a packing factor, is introduced to account for random distributions of semicylinders. The Twersky theory is based on the assumptions that the product of roughness size and wave number is very much less than unity, and the product of roughness separation distance and wave number is less than unity.

B. Sound propagation in long enclosures with a hard rough surface

Consider the situation for calculating the sound field due to a point source of unit strength radiating sound inside a rectangular enclosure. The sound field is composed of a direct contribution from the source and the contributions from image sources due to multiple reflections inside the enclosure (see Fig. 2). The total sound field at a receiver point can be computed by summing all contributions to give,[15]

$$P_{\text{tot}} = \frac{e^{ikr_d}}{4\pi r_d} + \frac{1}{4\pi}\sum_{n=0}^{N} Q_{sn}\frac{e^{ikr_n}}{r_n}, \tag{5}$$

where N is the maximum number terms used in the ray series and r_d and r_n are the distances of direct path and specularly reflected path with image source n from the receiver, respectively. Unless otherwise stated, the subscript n denotes the corresponding parameters for the image source n. In Eq. (5), a factor known as the combined complex wave reflection coefficient Q_{sn} is used. At each interaction with a boundary plane, the complex reflection coefficient Q_n is determined according to

$$Q_n = R_n + (1-R_n)F(w_n), \tag{6a}$$

where the plane wave reflection coefficient R_n is given by

$$R_n = (\cos\alpha_n - \beta_n)/(\cos\alpha_n + \beta_n), \tag{6b}$$

the boundary loss factor $F(w_n)$ is calculated by

$$F(w_n) = 1 + i\sqrt{\pi}w_n e^{-w_n^2}\,\text{erfc}(-iw_n), \tag{7}$$

w_n is the numerical distance determined by

$$w_n = \sqrt{\tfrac{1}{2}ikr_n}(\cos\alpha_n + \beta_n), \tag{8}$$

β_n is the specific normalized admittance of the reflecting plane, and α_n is the incident angle of the reflected wave. The successive reflections of a sound wave is then modeled as the multiplication product for all the associated Q_n of the image source n, i.e., the complex wave reflection coefficient is multiplied each time when the reflected wave interacts with a boundary surface. The combined complex wave reflection factor is denoted by Q_{sn} in Eq. (5).

The specific normalized admittance β_n is zero if the reflecting surface is a hard smooth plane. On the other hand, if the reflected wave hits the rough surface, then β_n is calculated according to Eqs. (1)–(4). With the use of Eq. (5), the sound field for the propagation of sound due to the presence of rough surfaces inside a long enclosure can be computed.

C. The effect of semicylindrical bosses on sound propagation in tunnels

To investigate the effect of the hard rough surfaces inside a tunnel, it is useful to examine the spherical wave reflection coefficients Q_n for each interaction with the rough surface. It is noted that the modified admittance β_n is different because of the fact the incident and azimuthal angles are different for different image sources. With different values of β_n, the plane wave reflection coefficients R_n and the spherical wave reflection coefficients Q_n are all different. However, both the plane wave reflection and spherical wave reflection coefficient become 1 when β_n tends to zero (i.e., for a hard smooth surface).

According Eq. (1), the Twersky's boss model predicts a nonzero real part η_{2D} for the effective admittance of a hard rough surface. Physically, this "loss" term may be attributed to the infinitesimal viscous losses due to heat convection occurred on the layer between the boss' surface and the atmosphere upon the multiple incoherent scattering of waves between neighboring rigid bosses and the rigid plane. The hard rough surfaces can also be interpreted as the presence of diffusely reflecting surfaces and Kang[1] has demonstrated the effectiveness of using diffusely reflecting surfaces (without increasing absorption) to reduce noise in long spaces.

The apparent "absorptiveness" of a rough surface can be examined by investigating the dependency of the magnitudes of plane wave reflection coefficient with the angle of incident at various azimuthal angles for the reflected waves. Figures 3(a)–3(d) show variations of $|R_p|$ with α for different azimuthal angles (0°, 15°, 30°, 45°, 60°, 75°, and 90°, respectively) with the radius of the semicylindrical bosses a of 0.08 m for cases (a) and (b) and of 0.04 m for cases (c) and (d). The average center-to-center spacing between semicylindrical bosses b varies from $4a$ to $5a$. In Figs. 3(a) and 3(c), the predicted $|R_p|$ are shown for the minimum center-to-center spacing between two adjacent semicylindrical bosses of $3.5a$ (dotted line) and of $3a$ (solid line). In Figs. 3(a) and 3(b), the predicted $|R_p|$ are shown for the minimum center-to-center spacing between two adjacent semicylindrical bosses of $4.5a$ (dotted line) and of $4a$ (solid line).

The source frequency used in the graphs is 500 Hz which means that the plots with $ka=0.74$ are shown in Figs. 3(a) and 3(b) and with $ka=0.37$ are shown in Figs. 3(c) and 3(d).

The magnitude of the reflection coefficient is equal to 1 when the reflected wave is propagated at the grazing angle, $\alpha=\pi/2$. The magnitude of the reflection coefficient is also

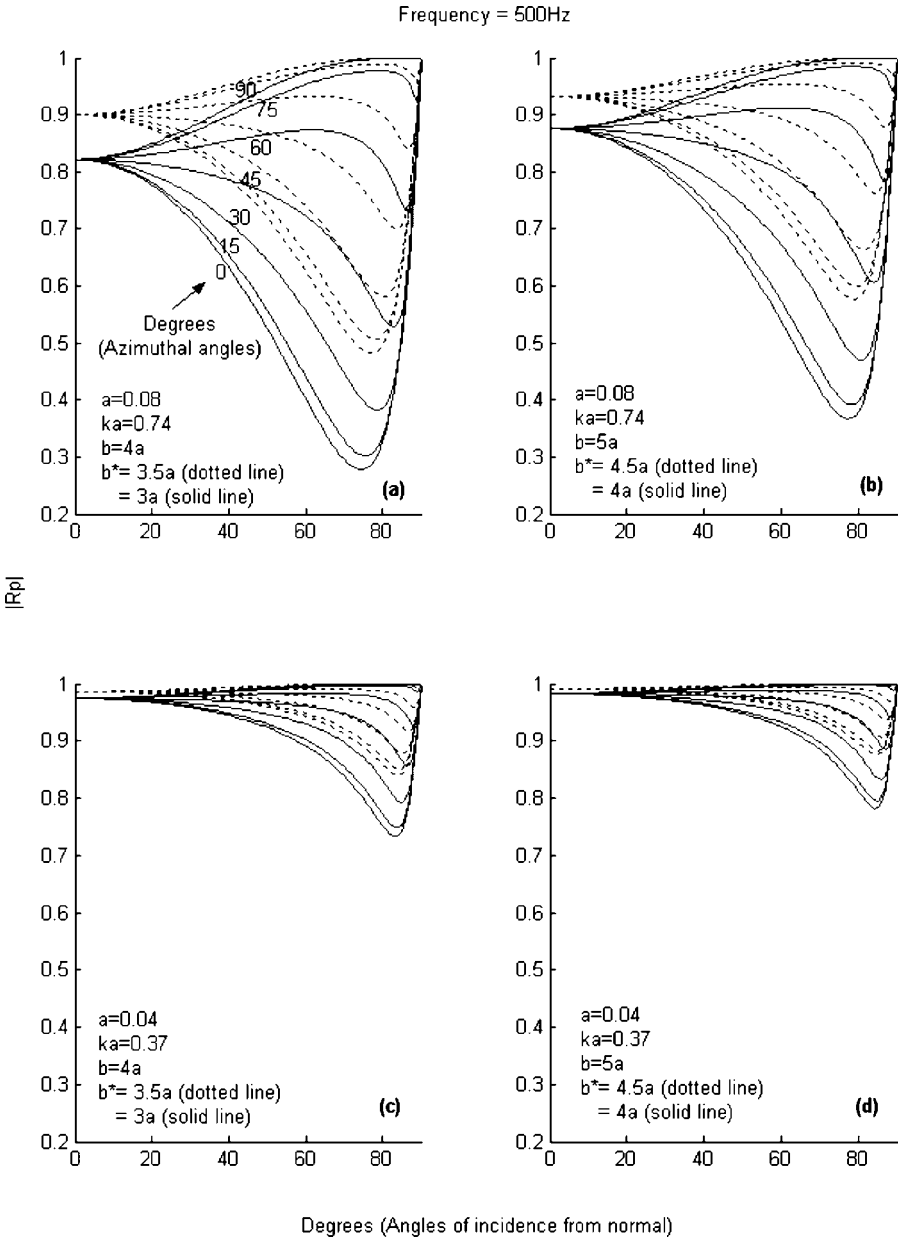

FIG. 3. Predicted variations of $|R_p|$ with the angle of normal incidence, the azimuthal angles of the incident wave, and different roughness parameters.

independent of the azimuthal angle when the reflected wave approaches the rough surface at the normal incidence, i.e., $\alpha=0$. Substituting $\alpha=0$ into Eqs. (1)–(3) and, in turn, into Eq. (6b), $|R_p|$ can be determined as follows:

$$|R_p| = \frac{\sqrt{[1 - mk^3\pi^2a^4(1 - W^2)/8]^2 + [kV]^2}}{\sqrt{[1 + mk^3\pi^2a^4(1 - W^2)/8]^2 + [kV]^2}}. \quad (9)$$

From Fig. 3(a)–3(d), we see that $|R_p|$ decreases when α increases from 0 until it reaches a minimum value before it increases to 1 when $\alpha=\pi/2$. We can see from Fig. 3(a) that $|R_p|$ has a value of as low as about 0.3 for a azimuthal angle of 0° and an incident angle of around 75°.

Comparison of predictions using different roughnesses with $a=0.08$ m in Fig. 3(a) and with $a=0.004$ m in Fig. 3(c) show that more absorption is expected for the surface with higher value of a, i.e., surface with more roughness. In addition, Figs. 3(a) and 3(b) compare $|R_p|$ with two average center-to-center distances ($b=4a$ and $5a$). It can be seen from these two plots that the closer the separations between two adjacent bosses, the larger the predicted effect of the modified admittance, i.e., more apparent "absorption." The degree of nonperiodicity distributions of semicylindrical bosses leads to a larger absorptive effect due to the modified admittance. This effect is shown in all plots of Fig. 3. We can see that use of surface roughness can lead to a certain degree of absorption when the sound waves are incident on a rough surface. Hence, we expect that the deployment of rough surfaces can lead to the reduction in the total sound field in long enclosures.

III. MODEL VALIDATIONS

It is remarkable that an incoherent scattering effect is expected by distributing semicylindrical rods nonperiodically [i.e., $W \neq 1$ in Eqs. (2) and (4)]. These semicylindrical rods were used to simulate a two-dimensional (2D) hard rough surface. Noting the approximation of small ka, the size of

roughness chosen for the current experimental means that the theoretical model for a rough surface should give valid predictions for frequencies up to about 4 kHz. A series of measurements with different source locations were conducted to confirm the Twersky model although extensive studies have been carried out elsewhere.[23]

Measurements were conducted at different receiver locations over a rough surface in the anechoic chamber with size of $6\times6\times4$ m^3 (high). The measured data were obtained to validate the Twersky boss model. The experimental setup is shown in Fig. 3. The rough surface is made of wooden semicylindrical rods embedded on a smooth wooden board. The radius of each semicylindrical rod is 0.015 m, which was fixed onto a 1.25-cm-thick plywood board with dimensions of 2.4×4.8 m^2. Prior measurements were conducted to measure the acoustic characteristic of the plywood board. We found that the plywood board could generally be treated as a perfectly reflecting plane. The semicylindrical rods were assumed to be acoustically hard because they were also made by the same material as the plywood board. The semicylindrical rods and the plywood board were varnished to prevent the leakage of sound. The semicylindrical rods were spaced pseudorandomly with an average distance and a minimum center-to-center separation between two adjacent semicylinders of 0.06 and 0.0525 m, respectively.

A Tannoy speaker, which was fitted on a long brass pipe of 1 m long and 25 mm in diameter, was used to simulate an omnidirectional point source. Preliminary measurements were conducted to examine the directional characteristic of the point source. The measured result, not shown here for brevity, suggests that the deviation in the directivity pattern for all directions is within 1 dB for all frequencies above 250 Hz.

For the measurements, the point source and receiver were located at various positions over the rough surface. A Bruel & Kjaer type 4942 microphone (prepolarized, diffuse field), fitted with a Bruel & Kjaer type 2671 preamplifier and a Bruel & Kjaer NEXUS conditional amplifier, was used as a receiver. The microphone was placed at various heights above the floor by mounting it on an adjustable stand. A special type of test signal called a maximum length sequence (MLS) was employed to obtain the experimental data. The deterministic nature of the MLS provides an excellent signal-to-noise ratio, which was ideal for the current indoor experiments. The MLS signals were generated by the maximum length sequence signal analyzer (MLSSA) 2000 card, transferred via the built-in digital-to-analog-converter and boosted by a Bruel & Kjaer 2713 power amplifier. The MLS signals were then connected to the Tannoy speaker, which emitted sound for experiments. The measurements were recorded in the time domain. Manipulations of time-domain measured signals were possible for eliminating unwanted reflections.

We introduce a term known as the excess attenuation (EA) to facilitate the presentation of the measured results. EA is the difference in sound pressure levels with and without the presence of the rough surface, i.e.,

$$\mathrm{EA} = 20\log_{10}(P_{\mathrm{tot}}/P_{\mathrm{ff}}), \tag{10}$$

where P_{tot} is the total sound field above the rough surface and P_{ff} is the corresponding free field sound pressure at the same receiver location without the presence of any reflecting surface.

The results predicted by the Twersky boss model are subsequently compared with that evaluated by a wave-based numerical formulation. As the geometrical configuration of the current situation is an external problem, the boundary element method[28] (BEM) is an appropriate approach for the purpose of validation for both indoor measurements and the boss model. The BEM formulation has been extensively used to study the physical phenomenon of outdoor sound propagation in an irregular terrain. In the BEM study, the rough surface is partitioned with at least ten elements per wavelength, and each individual semicylindrical boss was represented by seven elements. In the BEM formulation, a FORTRAN program was used to solve the set of simultaneous equations by using the standard matrix method. The computational time for the BEM formulation will increase exponentially for higher source frequency and for a larger source/receiver separation. On the other hand, a simple MATLAB program was developed for the Twersky's boss model which was then used to predict the propagation of sound above the hard rough surface.

Three receiver locations are chosen for comparison. Both source and receiver are located 0.2 m above the bottom of rough surface and with horizontal distances of (a) 1 m, (b) 2 m, and (c) 3 m. In each plot [Figs. 4(a)–4(c)], comparisons of the measurements (dotted lines with symbols) and predictions using the BEM formulation (dashed lines) and the image source model (solid lines) are shown. The effect of atmospheric absorption is ignored in all the numerical predictions.

Comparing the smooth and rough reflecting planes, Figs. 4(a)–4(c) show that there are significant shifts of main ground effect dips to the low frequency for a rough surface. From the measured data and the numerical predictions, it is shown that the plywood board can be treated essentially as a rigid reflecting plane. For the hard rough cases, predictions according to Twersky's model show reasonably good agreement with the measured data and with the predictions using BEM formulation at various locations. It is reassuring to confirm that Twersky's boss model can provide an accurate prediction of the scattering effects due to a hard rough surface.

A model rough surface, which was now built for the next experimental study, was placed either in an indoor enclosure or in a larger outdoor-modeled tunnel. The measured data were obtained to validate the image source model for the propagation of sound over a rough surface in a tunnel.

For the indoor case, we conducted a series of measurements with the use of an enclosure of 4.8 m long which was placed in the anechoic chamber. The enclosure was

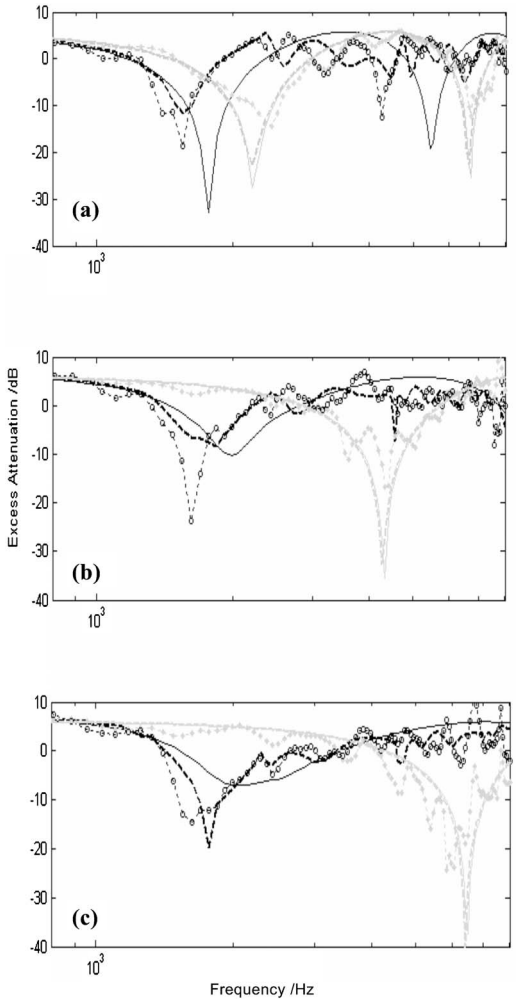

FIG. 4. Comparisons of measured (symbols) and predicted (lines) excess attenuation spectra from a point source over a plywood board with and without semicylindrical bosses. Both source and receiver are located 0.2 m above the plane and with horizontal distances of (a) 1 m, (b) 2 m, and (c) 3 m. Dotted line with circles, measurements (rough), dotted line with stars, measurements (smooth); dashed lines (black), BEM predictions (rough); dashed lines (gray), BEM predictions (smooth); solid lines (black), Twersky's boss model; and solid lines (gray), coherent image source method.

constructed with a rectangular cross section of 1 m wide and 1.2 m high. The four boundary surfaces of the enclosure were made of plywood with flat surfaces. To model the scattering effect due to the roughness of the enclosure's surface, the entire length of the left vertical wall was installed with semicylindrical wooden rods of 0.015 m radius. These semicylindrical rods were distributed pseudorandomly with a minimum center-to-center separation of 0.0525 m. This arrangement ensures that the assumption of small *ka* can be met that, in turn, allows valid numerical predictions for frequencies up to about 4 kHz. The experimental setup is shown in Fig. 5.

Measurements of sound propagation along the enclosure using the same set of measuring equipment are described earlier. However, we present the experimental data in term of the relative sound pressure level (RSL), which is defined as

FIG. 5. An experimental setup in an anechoic chamber for measurement of sound propagation in a long enclosure with a roughening surface on the left vertical wall. Semicylindrical wooden rods of 0.015 m radius were taped securely on the wooden board. The rods were distributed pseudorandomly with a minimum center-to-center separation between two adjacent semicylinders b^* of 0.0525 m.

$$\mathrm{RSL} = 20 \log_{10} \left| \frac{P_{\mathrm{tot}}}{P_{\mathrm{ref}}} \right|, \tag{11}$$

where P_{ref} is the reference free field sound pressure measured at a horizontal distance of 1 m in front of the source. It is more convenient to use the relative sound pressure level in favor of the excess attenuation because it is generally more difficult to obtain free field measured level for the receiver placed over 2 m from the source.

Both the source and receiver were located along the center line of the enclosure and 0.6 m above the floor in the first set of measurements. They were then placed at two offset points: 0.75 and 0.25 m from left vertical wall (installed with semicylindrical rods) with the respective heights of 0.3 and 0.6 m. The experimental data were taken at various horizontal distances in front of the source. The setup is shown in Fig. 5. A separate measurement of the reference sound pressure level was carried out at a horizontal distance of 1 m from the source in the anechoic chamber without the presence of any reflecting surfaces. The background noise level was sufficiently low to provide a reference signal for use in subsequent experimental measurements.

In the computations, as can be seen in Fig. 2, the determination of image source location is followed by using the image source model according to Li and Iu.[15] For the case of hard surface, it can be seen from Eq. (5) that the rectangular enclosure contains an infinite number of image sources due to the presences of ceiling, floor, and two wall surfaces on the left and right sides. Preliminary numerical analyses were conducted. It is found that the series given in Eq. (5) normally converge for about 50 terms. The number of terms N

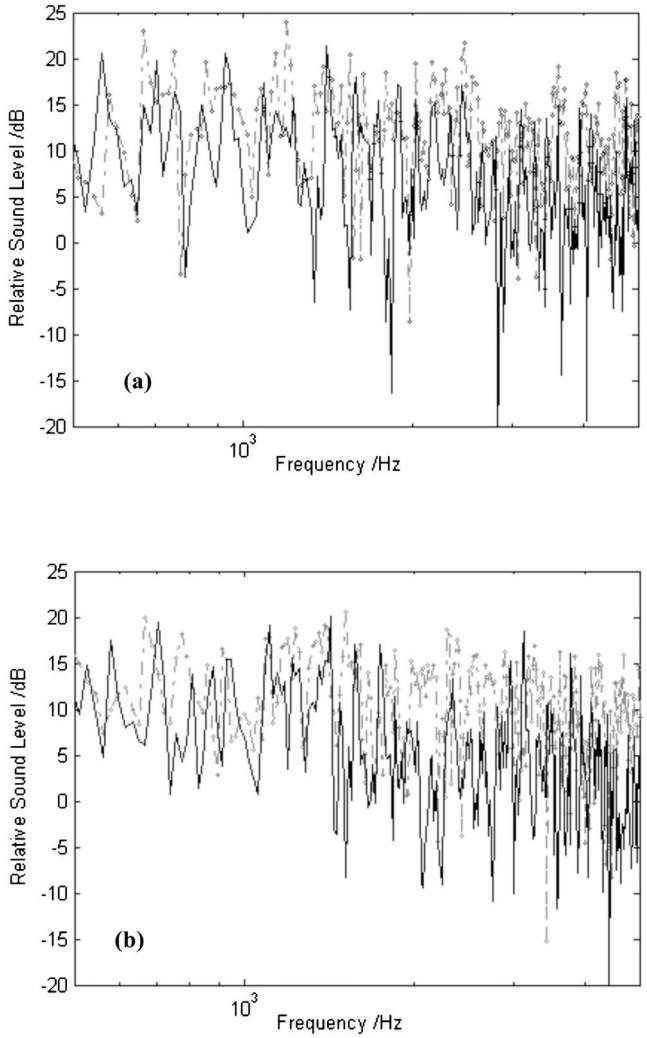

FIG. 6. Comparison of measured (solid line) and predicted (dashed-dotted line with diamonds) relative sound pressure level in a scale model enclosure built in an anechoic chamber with hard boundaries. Semicylindrical rods (a=0.015 m, length=1.2 m, b=0.06 m, b^*=0.0525 m) were taped on to the left vertical surface to form a 2D hard roughness surface. The source and receiver were both located at the center line (0.5 m from either vertical walls) and their heights were 0.6 m above the floor. The horizontal separations between source and receiver were (a) 1 m, and (b) 2 m.

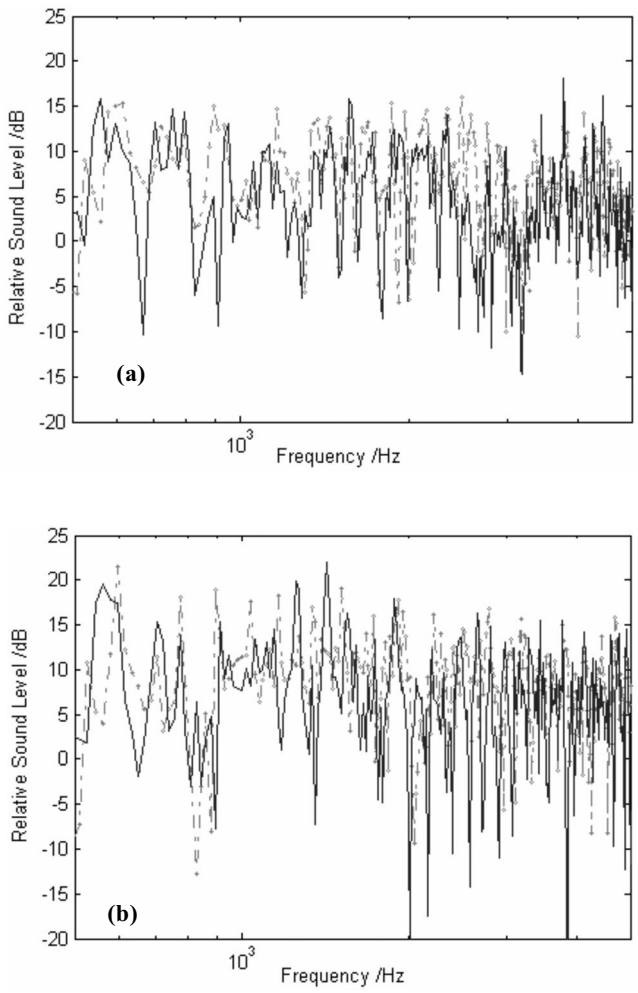

FIG. 7. Same as Fig. 6, except that the source was located at an offset position (0.75 m from the left vertical wall) and the height at 0.3 m. The receiver was also located at an offset position (0.25 m from the left vertical wall) and the height at 0.6 m. The same horizontal separations between source and receiver were used with (a) 1 m and (b) 2 m.

required to ensure the convergence of the ray series depends on the geometrical configuration and the effective impedance of the tunnel surfaces. We do not attempt to optimize the choice of N but simply choose the variation of the magnitude of the reflected waves for two consecutive terms is less than 1%. This condition has proven to be adequate for the image source model to give satisfactory numerical results.

In Figs. 6 and 7, the predicted RSL are shown in which the Twersky model is used in conjunction with Eq. (5) for the numerical models. Both measured and predicted results show a regular pattern of "dips" and "peaks" in the frequency spectra. Both spectra fluctuate considerably as the frequency increases. This phenomenon corresponds to destructive and constructive interferences of the contributory rays. Although there are noticeable discrepancies in the magnitudes of peaks and dips between the measured and predicted RSL, the trends in the frequency spectra agree reasonably well with each other. The interference pattern of the RSL spectra suggests that the phase information of each ray plays an important role in predicting the total sound field in the enclosures. As mentioned in our early studies,[15,16] the energy-based incoherent model will not be adequate to predict the sound fields in the tunnels.

We further remark that the locations of dips and peaks in the spectrum are sensitive to the small change in the source/receiver geometry especially at high frequencies. According to Fig. 6(b), there are several distinct peaks predicted above 2000 Hz but these peaks are not matched with the measured results. Indeed, the patterns of fluctuations in the frequency spectra are quite different for the measured and predicted results. These apparent discrepancies are largely due to the imprecise location of the receiver relative to the source in the tunnel. A small error in the position can lead to predictions of a significant phase shift for the contribution from a ray. This is particularly noticeable for high frequencies and large distances as was shown in comparable results of our previous studies in long enclosures[15–17].

Next, we illustrate the effect of a hard rough surface in tunnels by comparing the sound fields for a hard "smooth" tunnel. The insertion loss (IL) is used in the following presentation, where

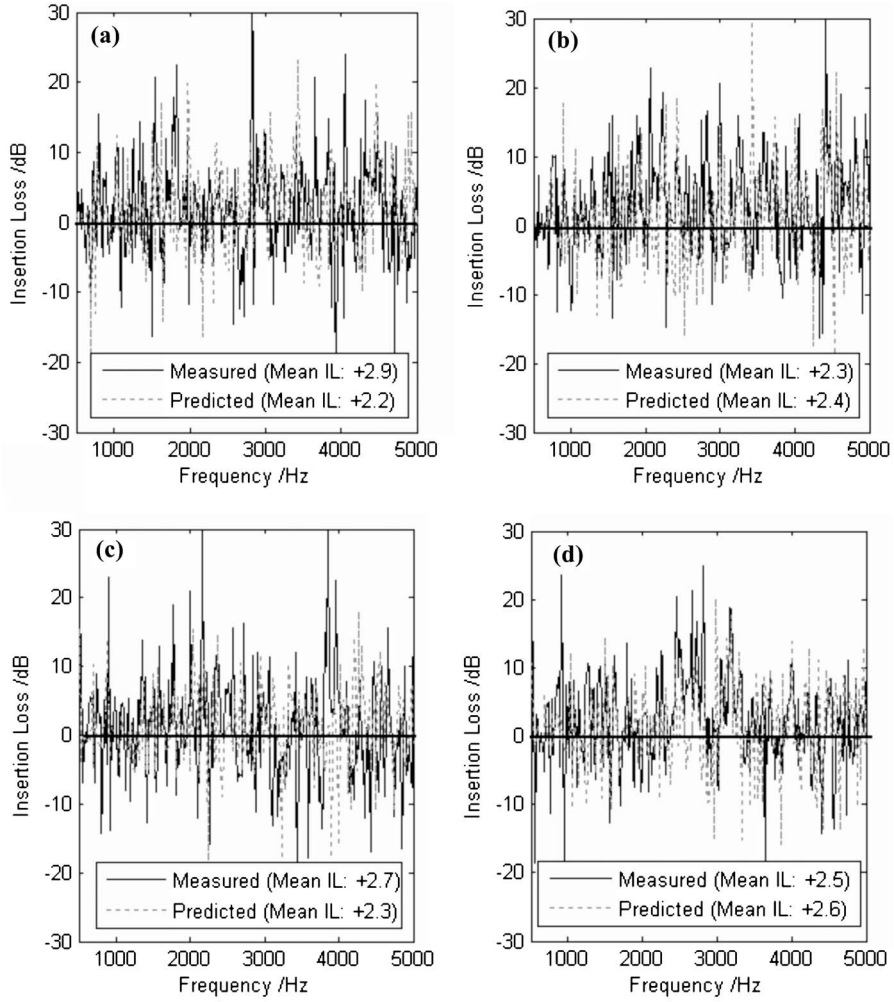

FIG. 8. The insertion loss (IL) spectra at different source/receiver locations with left vertical surface having 2D hard semicylindrical rods in the scale model enclosure over surface with smooth hard condition. The dotted line represents predictions by the complex image source model. The solid line represents results from experimental measurement: [(a) and (b)] source and receiver locations correspond to Figs. 6(a) and 6(b); [(c) and (d)] source and receiver locations correspond to Figs. 7(a) and 7(b), respectively. The mean values of measured and predicted IL over the frequency spectrum are also indicated.

$$\mathrm{IL} = 20 \log_{10}\left(\left| \frac{p_{\mathrm{w/o}}}{p_{\mathrm{w}}} \right| \right), \tag{12}$$

p_{w} and $p_{\mathrm{w/o}}$ are the total sound fields with or without the rough surface in the tunnel, respectively. Figure 8 shows the comparisons of the predicted ILs with experimental data for four receiver locations. Both the predicted and measured ILs fluctuate considerably over the frequency range with consistent agreements on the peak and dip locations. The mean value of measured IL ranges between 2.3 and 2.9 dB. The mean value of the predicted IL ranges between 2.2 and 2.6 dB. Introducing a hard rough surface on one of the vertical walls of the scale model tunnel can lead to an average reduction in the noise levels of about 3 dB over the frequency range from 500 to 5000 Hz.

Another series of measurements have been conducted in a larger model tunnel with a scale of 1:10. The tunnel, which was placed outdoors, was made of gypsum boards with an internal cross sectional area of $1.16 \times 1.46\ \mathrm{m}^2$. The tunnel was 27 m long with an anechoic termination constructed at one end. The MLSSA measurement system was again used. A Renkus-Heinz PN61 loudspeaker was used as a point source in this case to provide a higher sound power. Plywood boards were covered along the left vertical wall of the model tunnel. Varnished wooden rods of semicylindrical shape of 1.4 m long with radius 0.015 m were taped securely onto these plywood boards to form a 2D hard rough surface.

The semicylindrical rods were pseudorandomly spaced and distributed vertically on the left side wall with a minimum center-to-center separation of 0.04 m. To investigate the spatial variations of the sound field, two sets of source/receiver geometries were selected for measurements. For the first set of measurements, the source was located along the center line of the outdoor model tunnel. It was then placed at an offset position of 0.86 m from the left vertical wall for the second set of measurements. Two separate source heights of 0.8 and 0.4 m above the floor were chosen for these two sets of experimental measurements. The receivers were located at different positions along the center line with the horizontal separations of 2, 5, and 10 m from the source.

Since the gypsum boards were used for the construction of this outdoor model tunnel walls, the assumption of perfectly reflecting surfaces led to inaccurate predictions of the total sound fields in the enclosure. Hence, the characterization of the acoustical impedance of the gypsum boards was essential because of contributions from the reflected sound fields are one of the major components for the present situation. An impedance deduction method[26] was used to determine the acoustical characteristics of the gypsum boards. It was also found that a two-parameter impedance model[27] was

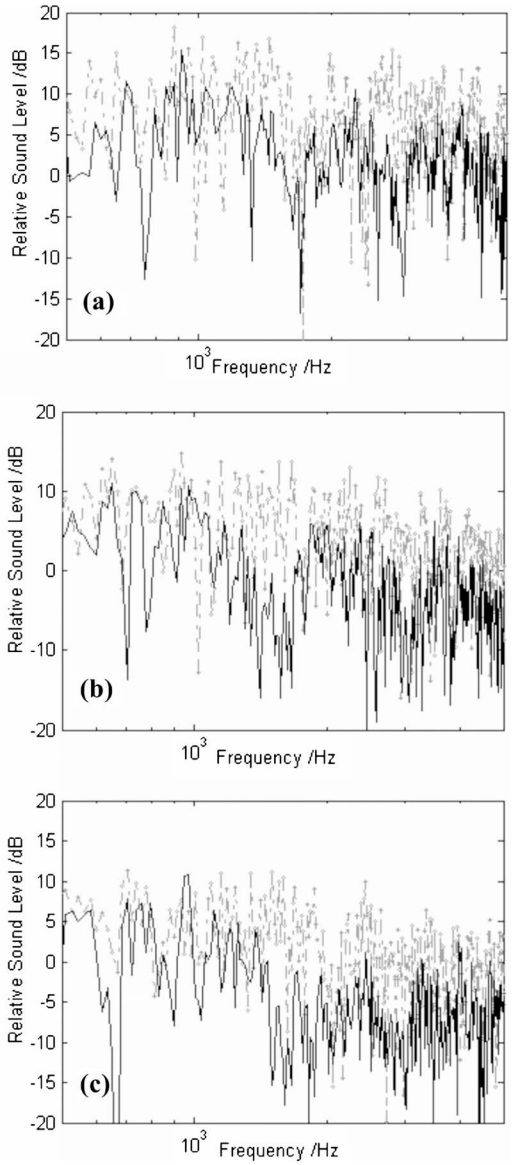

FIG. 9. (Color online) Comparison of measured (solid line) and predicted (dashed-dotted line with diamonds) relative sound pressure level in the outdoor model tunnel. Semicylindrical rods (a=0.015 m, length=1.4 m, b =0.045 m, b^*=0.04 m) were taped securely on the left vertical wall of the tunnel to form a 2D hard roughness surface. The source and receiver were both located at the center line (0.58 m from either wall) and both heights were 0.8 m. The horizontal separations between the source and receiver were (a) 2 m, (b) 5 m, and (c) 10 m.

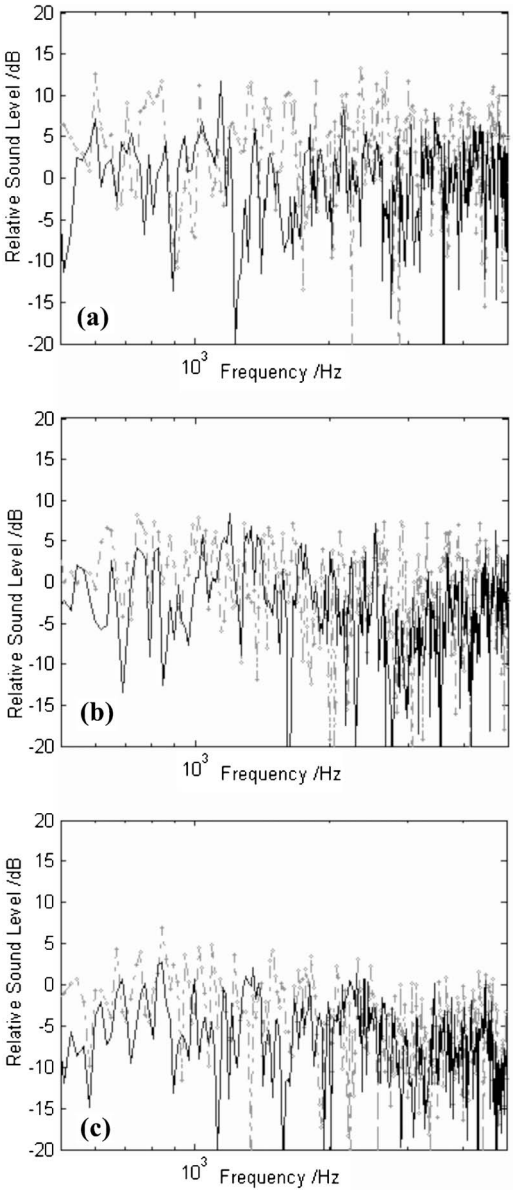

FIG. 10. Same as Fig. 9, except the source and receiver were located at the offset position (0.86 m from the left vertical wall) and the centre line, respectively. The height of the source was 0.4 m and it was 0.8 m above the floor for the receiver. The horizontal separations between the source and receiver were the same at (a) 2 m, (b) 5 m, and (c) 10 m.

sufficiently accurate to represent its acoustical impedance. The effective flow resistivity of 6000 kPa s m^{-2} and the effective rate of change in porosity with depth of 100 m^{-1} were deduced from the measurements in the present study. These parametric values are then used in the subsequent prediction of the sound field in the model tunnel.

Next, we show comparisons of the frequency spectra of the measured and predicted RSL in the model tunnel. Figures 9 and 10 display the measured results for the source and receiver located at the center and offset positions respectively. A clear pattern of dips and peaks, which are similar to the earlier indoor measurements, is evinced in these two plots. In comparing both measured and predicted results, it can be seen that general agreements between measurements and predictions at different receiver positions are obtained.

However, as shown in Fig. 9, the patterns of the predicted and measured frequency spectra show some notable discrepancies when the source and receiver were located along the center line of the model tunnel. Again, these apparent discrepancies are possibly due to the phase errors of contributory rays as discussed earlier for the results of the indoor scale model enclosure. On the other hand, when the source and receiver were located at the offset positions (see Fig. 10), the predicted spectra show better agreement with the measured results.

We remark that the measured and predicted results for a tunnel with smooth hard walls were presented elsewhere.[15] Their results showed that the complex image source method agrees reasonably well with experimental data. Hence, in

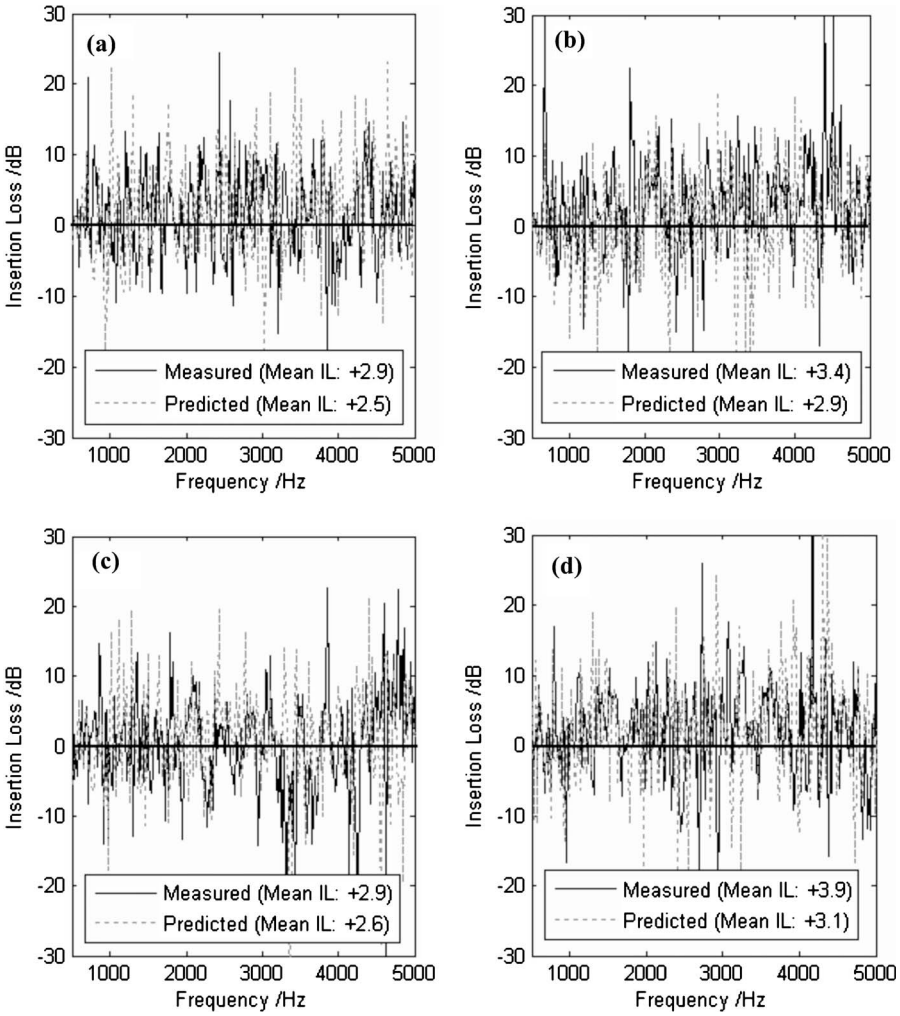

FIG. 11. The insertion loss (IL) spectra at different source/receiver locations with left vertical surface having 2D hard semicylindrical rods in the outdoor model tunnel over surface with smooth hard condition. The dotted line represents predictions by the complex image source model. The solid line represents results from experimental measurement: [(a) and (b)] source and receiver locations correspond to Figs. 9(a) and 9(b); [(c) and (d)] source and receiver locations correspond to Figs. 10(a) and 10(b), respectively. The mean values of measured and predicted IL over the frequency spectrum are also indicated.

Fig. 11, we only compare the predicted insertion loss (IL) with experimental data for four receiver locations. The predicted IL and measured IL, which agree reasonably well for the peak and dip locations, fluctuate considerably over the frequency range of interest. The average value of measured IL ranges between 2.9 and 3.9 dB and it is between 2.5 and 3.1 dB for the predicted IL.

With the measured data at the two model tunnels, it is possible to conclude that the application of the Twersky model for a rough surface in the coherent model is capable to predict the influence of surface roughness on the propagation of sound in long enclosures. Introducing a hard rough surface on one of the vertical walls of the model tunnels can lead to an average reduction in the noise levels of about 3 dB over the frequency range from 500 to 5000 Hz.

IV. APPLICATION—NOISE REDUCTION IN LONG ENCLOSURES BY ROUGH SURFACES

We have validated experimentally in an indoor enclosure and a model tunnel that effective impedance can be introduced on the wall by embedding arrays of semicylindrical bosses on an otherwise smooth and hard boundary surface. The coherent model can be used to predict the propagation of sound in tunnels. It is apparent that the surface roughness can lead to the reduction in the reverberant sound fields by introducing effective impedance on the tunnel walls. This implies that roughening of an otherwise acoustically hard surface may help to provide a passive noise control in tunnel environments.

In this section, we consider an example for noise reduction in a tunnel due to multiple sources. We endeavor to simulate the situations of using a hard rough surface to reduce the overall noise levels in the tunnel. The case chosen in this study emulates a common urban situation where there are many vehicular sources in a tunnel for road traffic. It is noted that the multiple sources were considered in this simulation instead of a simple line source. It is because a relatively large separation distance between adjacent vehicles is expected in most practical situations.

Here, the total sound pressure level L_T due to a total of N_s vehicular sources can be determined straightforwardly as follows:

$$L_T = 10 \log_{10} \sum_{j=1}^{N_S} 10^{\mathrm{SPL}_j/10}, \tag{12'}$$

where SPL_j is the contribution from the jth image source. We remark that the total sound pressure level at a receiver point is obtained by first summing the contributions from all images for each source coherently. The overall L_T is then calculated by adding the contributions from all individual sources incoherently.

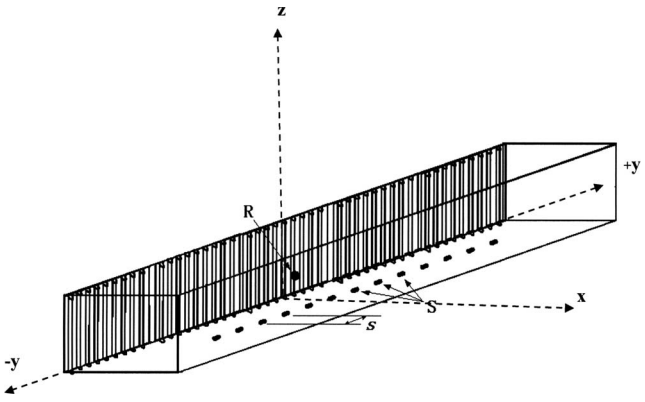

FIG. 12. A model road traffic tunnel use in the numerical simulations.

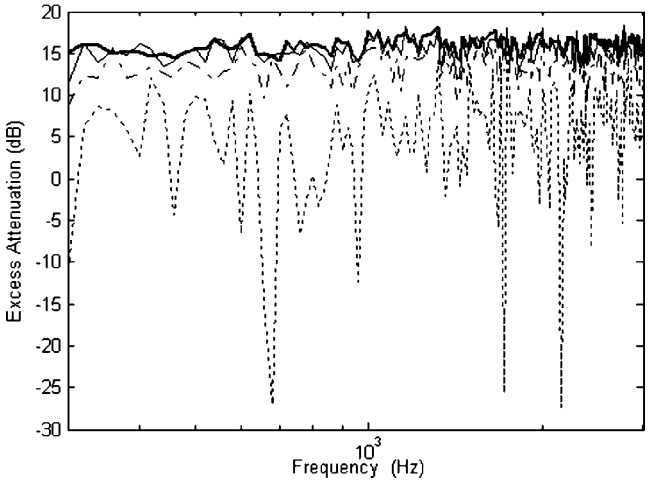

FIG. 13. Predicted excess attenuation in a road traffic tunnel with hard surfaces. (Thick solid line, $s=5$ m; thin solid line, $s=10$ m; dash-dotted line, $s=20$ m; and dotted line, single source).

The objective of this example is to quantify the sound amplification due to the effect of multiple reflections and to assess the sound reduction by deploying a hard rough surface on one side of the tunnel walls. Modeling this situation, we assume that the source and receiver are located inside an infinitely long tunnel with a constant cross-sectional area of rectangular in shape. To facilitate the numerical analysis, a rectangular coordinate system is used, where the origin is located at the bottom left corner of the tunnel (see Fig. 12). The cross section of the tunnel has a dimension of 8 m wide (x direction) and 10 m high (z direction). The tunnel is extended to infinity at both directions along the y axis and the receiver is located at the plane of $y=0$. Suppose a number of concrete blocks of semicylindrical shape with radius of 0.075 m were constructed to form a 2D hard rough surface on one side of the tunnel walls. The concrete blocks are spaced and distributed on the left vertical wall with average separation of 0.3 m. The minimum center-to-center separation between two adjacent semicylinders is 0.2 m. We treat all other boundaries, i.e., the ground, the ceiling, and the right side vertical wall, as perfectly reflecting surfaces. This assumption is justifiable because most surfaces in a tunnel environment are acoustically hard.

The cases of a single source and multiple sources are considered in the following numerical simulations with the receiver placed at (2, 0, 4). For the first simulation, a single source is located at (4, 0, 0.5). For the second case, a series of multiple sources are placed at a height of 0.5 m above the ground and 4 m along the center line of the tunnel. Three separations between two adjacent sources (labeled as s in Fig. 12) are considered with the respective distances of 5, 10, and 20 m along the y axis. In our preliminary analysis, it is found that contributions from any sources which are located at a horizontal distance more than 100 m from the receiver are negligible when their contributed noise levels are compared with those due to the nearer sources.

Figure 13 displays numerical predictions of the sound pressure levels due to the single source and multiple sources. In the plots, the excess attenuation EA is used to present the predicted results where it is defined as the difference in the total sound pressure levels at a receiver point with (L_T) and without ($\bar{L}_T$) the presence of the tunnel, i.e.,

$$\mathrm{EA} = L_T - \bar{L}_T. \tag{13}$$

The predicted EA spectra for the two cases are presented in Fig. 13 for the source frequency ranging from 300 to 3000 Hz. For the case of a single noise source, it can be seen that the overall average sound pressure level is about 8 dB higher than the average free field sound pressure levels. For the case of multiple noise sources with 5 m separation, the overall average sound pressure level increase to about 16 dB above the average free field sound pressure level due to the multiple noise sources. The predicted results for other two separations (10 and 20 m) are rather similar to the results of the 5 m separation with the average EA of about 15 and 13 dB, respectively. For a single source, the predicted results confirm that there is a significant amplification of the overall sound pressure levels because of the effect of multiple reflections of the tunnel walls. The effect of multiple reflections becomes even more acute when there are multiple sources in the tunnel.

Finally, we show that the overall sound pressure levels can be reduced by deploying a 2D hard rough surface on one side of vertical wall inside the road tunnel. This is illustrated in the following numerical simulation. For the case of multiple sources with 5 m separation in the tunnel, Fig. 14 displays the predicted excess attenuation in the tunnel with and without the use of hard rough surface on one side of vertical wall inside the traffic tunnel. We can see that there is an average of about 12 dB above the free field sound pressure levels. This represents a reduction of 4 dB for the case without the presence of the rough surface. For the source and receivers at other locations, calculations show comparable levels of noise reduction. These numerical simulations are not shown here for brevity.

V. CONCLUSIONS

The Twersky boss formulation has been applied to the image source model for the calculation of the sound pressure levels in a rigid tunnel with the presence of a 2D hard rough surface on one of its vertical wall. The proposed theoretical model was validated by comparing with experimental measurements conducted in two model tunnels. The size of the

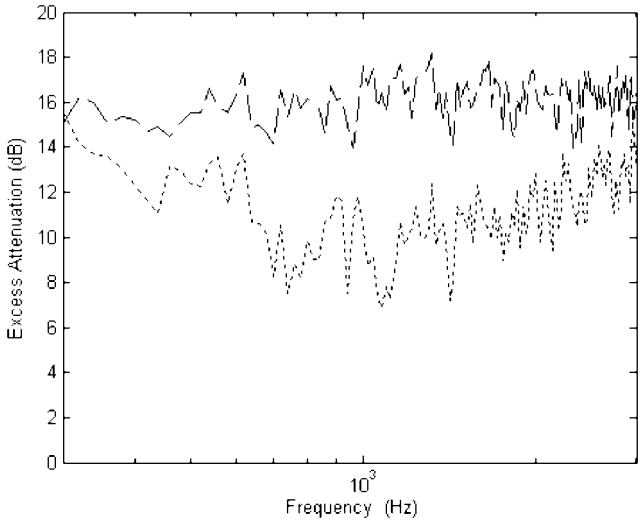

FIG. 14. Comparison of excess attenuation spectra in a road traffic tunnel with and without a hard rough surface: Dashes line, without roughness; dotted line, with roughness.

first model enclosure, which was placed in an anechoic chamber, was 1 m wide, 1.2 m high, and 4.8 meter long. The second tunnel was built with a scale of 1:10, which had a dimension of 1.16 m wide, 1.46 m high, and 27 m long. Comparing with experimental data, it was demonstrated that the presence of a hard rough surface on one of the vertical walls in the tunnel introduced effective impedance on the boundary. The presence of apparent impedance on the boundary surfaces led to the reduction in the average noise levels in an otherwise hard tunnel. In the scale model studies, it is found that the introduction of a hard rough surface on one of the vertical walls of the model tunnels can lead to an average reduction in the noise level of about 3 dB over the frequency range from 500 to 5000 Hz.

Numerical simulations have also been conducted for a traffic tunnel of a realistic size with a cross-sectional area of 6×8 m^2. Numerical simulations show that the sound pressure levels in the tunnel due a single noise source is about 8 dB above the free field sound pressure levels. For multiple noise sources operated in a tunnel, the sound pressure levels are predicted to be 16 dB higher than that of the free field sound pressure levels. The introduction of a hard rough surface on one of the vertical walls can lead to an average reduction in the noise level of 4 dB over the frequency range from 300 to 3000 Hz.

ACKNOWLEDGMENTS

The research described in this paper was financed jointly by the Innovation and Technology Commission of the Hong Kong Special Administrative Region and the Mass Transit Railway Corporation Limited, through the award of an Innovation and Technology Fund grant under the category of the University-Industry Collaboration Programme (Project No. UIM/39). The authors are grateful to William Fung, Chenly Lai, P M Lam, S T So, and T L Yip for their help in conducting the experiments. Part of the manuscript was prepared while one of the authors (M.K.L.) was a visiting scholar at Ray W. Herrick Laboratories, Purdue University.

[1] J. Kang, *Acoustics of Long Spaces: Theory Design and Practice* (Thomas Telford, London, 2002).
[2] J. Kang, "Modelling of train noise in underground stations," J. Sound Vib. **195**, 241–255 (1996).
[3] L. Yang and B. M. Shield, "The prediction of speech intelligibility in underground stations of rectangular cross section," J. Acoust. Soc. Am. **109**, 266–273 (2001).
[4] T. L. Redmore, "A theoretical analysis and experimental study of the behaviour of sound in corridors," Appl. Acoust. **15**, 161–170 (1982).
[5] J. Kang, "Acoustics in long enclosures with multiple sources," J. Acoust. Soc. Am. **99**, 985–989 (1996).
[6] S. J. van Wijngaarden and J. A. Verhave, "Prediction of speech intelligibility for public address systems in traffic tunnels," Appl. Acoust. **67**, 306–323 (2006).
[7] Research Committee of Road Traffic Noise in Acoustical Society of Japan, "ASJ prediction model 1998 for road traffic noise," J. Acoust. Soc. Jpn. **55**, 281–324 (1999).
[8] H. Imaizumi, S. Kunimatsu, and T. Isei, "Sound propagation and speech transmission in a branching underground tunnel," J. Acoust. Soc. Am. **108**, 632–642 (2000).
[9] J. Kang, "Reverberation in rectangular long enclosures with geometrically reflecting boundaries," Acust. Acta Acust. **82**, 509–516 (1996).
[10] M. V. Sergeev, "Scattered sound and reverberation on city streets and in tunnels," Sov. Phys. Acoust. **25**, 248–252 (1979).
[11] R. N. Miles, "Sound field in a rectangular enclosure with diffusely reflecting boundaries," J. Sound Vib. **92**, 203–226 (1984).
[12] J. Kang, "Reverberation in rectangular long enclosures with diffusely reflecting boundaries," Acust. Acta Acust. **88**, 77–87 (2002).
[13] K. K. Iu and K. M. Li, "The propagation of sound in street canyons," J. Acoust. Soc. Am. **112**, 537–550 (2002).
[14] J. Picaut, T. Le Pillès, P. L'Hermite, and V. Gary, "Experimental study of sound propagation in a street," Appl. Acoust. **66**, 149–173 (2005).
[15] K. M. Li and K. K. Iu, "Propagation of sound in long enclosures," J. Acoust. Soc. Am. **116**, 2759–2770 (2004).
[16] K. M. Li and P. M. Lam, "Prediction of reverberation time and speech transmission index in long enclosures," J. Acoust. Soc. Am. **117**, 3716–3726 (2005).
[17] P. M. Lam and K. M. Li, "A coherent model for predicting noise reduction in long enclosures with impedance discontinuities," J. Sound Vib. **209**, 559–574 (2007).
[18] V. Twersky, "Reflection and scattering of sound by correlated rough surfaces," J. Acoust. Soc. Am. **73**, 85–94 (1983).
[19] J. P. Chambers and Y. Berthelot, "Utilizing a modified impedance analogy on sound propagation past a hard, curved, rough surface," J. Acoust. Soc. Am. **1120**, 1186–1189 (2006).
[20] I. Tolstoy, "Coherent sound scatter from a rough interface between arbitrary fluids with particular reference to roughness element shapes and corrugated surfaces," J. Acoust. Soc. Am. **72**, 960–972 (1982).
[21] R. J. Lucas and V. Twersky, "Coherent response to a point source irradiating a rough plane," J. Acoust. Soc. Am. **76**, 1847–1863 (1984).
[22] K. Attenborough and S. Taherzadeh, "Propagation from a point source over a rough finite impedance boundary," J. Acoust. Soc. Am. **98**, 1717–1722 (1995).
[23] P. Boulanger, K. Attenborough, S. Taherzadeh, T. Water-Fuller, and K. M. Li, "Ground effect over hard rough surfaces," J. Acoust. Soc. Am. **104**, 1474–1482 (1998).
[24] P. Boulanger, K. Attenborough, and Q. Qin, "Effective impedance of surfaces with porous roughness: Model and data," J. Acoust. Soc. Am. **117**, 1146–1156 (2005).
[25] C. F. Chien and W. W. Soroka, "Sound propagation along an impedance plane," J. Sound Vib. **43**, 9–20 (1975).
[26] S. Taherzadeh and K. Attenborough, "Deduction of ground impedance from measurements of relative SPL spectra," J. Bone Jt. Surg., Am. Vol. **105**, 2039–2042 (1999).
[27] K. Attenborough, "Acoustical characteristics of rigid fibrous absorbents and granular materials," J. Bone Jt. Surg., Am. Vol. **73**, 785–799 (1983).
[28] S. N. Chandle-Wilde and D. C. Hothersall, "Efficient calculation of the green function for acoustic propagation above a homogeneous impedance plane," J. Sound Vib. **180**, 705–724 (1995).